Available online at www.sciencedirect.com

ScienceDirect

Advances in Space Research 56 (2015) 1015–1029

ADVANCES IN SPACE RESEARCH (a COSPAR publication)

www.elsevier.com/locate/asr

GNSS satellite geometry and attitude models

O. Montenbruck [a,*], R. Schmid [b], F. Mercier [c], P. Steigenberger [a], C. Noll [d], R. Fatkulin [e], S. Kogure [f], A.S. Ganeshan [g]

[a] Deutsches Zentrum für Luft- und Raumfahrt (DLR), German Space Operations Center (GSOC), 82234 Weßling, Germany
[b] Technische Universität München, Deutsches Geodätisches Forschungsinstitut (DGFI-TUM), Arcisstr. 21, 80333 München, Germany
[c] Centre National d'Etudes Spatiales (CNES), 18, avenue Edouard Belin, 31401 Toulouse Cedex 9, France
[d] Goddard Space Flight Center (GSFC), Code 690.1, Greenbelt, MD 20771, USA
[e] ISS-Reshetnev, 52, Lenin Street, Zheleznogorsk, Krasnoyarsk region, 662972, Russia
[f] Japan Aerospace Exploration Agency (JAXA), Tsukuba Space Center, 2-1-1 Sengen, Tsukuba-shi, Ibaraki 305-8505, Japan
[g] Indian Space Research Organization (ISRO), ISRO Satellite Center (ISAC), Bangalore 560 017, India

Received 6 May 2015; received in revised form 17 June 2015; accepted 18 June 2015
Available online 26 June 2015

Abstract

This article discusses the attitude modes employed by present Global (and Regional) Navigation Satellite Systems (GNSSs) and the models used to describe them along with definitions of the constellation-specific spacecraft body frames. A uniform convention for the labeling of the principal spacecraft axes is proposed by the International GNSS Service (IGS), which results in a common formulation of the nominal attitude of all GNSS satellites in yaw-steering mode irrespective of their specific orbit and constellation. The conventions defined within this document provide the basis for the specification of antenna phase center offsets and variations in a multi-GNSS version of the IGS absolute phase center model in the ANTEX (antenna exchange) format. To facilitate the joint analysis of GNSS observations and satellite laser ranging measurements, laser retroreflector array coordinates consistent with the IGS-specific spacecraft frame conventions are provided in addition to representative antenna offset values for all GNSS constellations.

Keywords: GNSS satellites; Attitude models; Antenna offsets; ANTEX; SLR

1. Introduction

The geometry and orientation (or, "attitude") of navigation satellites are critical information for the processing of observations from Global (and Regional) Navigation Satellite Systems (GNSSs) in precise orbit determination and precise point positioning applications (Kouba and Héroux, 2001). While orbit information is typically referred to the spacecraft center-of-mass (CoM), the navigation signals emerge from an antenna at a different location. The antenna position relative to the CoM, or, more generally, the phase center offsets (PCOs) and variations (PCVs; Schmid et al., 2005, 2007), are naturally specified in a body-fixed spacecraft coordinate system. Based on the CoM location and the orientation of the body axes relative to a terrestrial or celestial reference frame, the actual antenna position can be described in the required reference frame. The same considerations apply for the location of laser retroreflector arrays (LRAs), which are used on numerous navigation satellites for the purpose of satellite laser ranging (SLR).

* Corresponding author.
E-mail addresses: oliver.montenbruck@dlr.de (O. Montenbruck), schmid@tum.de (R. Schmid), flavien.mercier@cnes.fr (F. Mercier), peter.steigenberger@dlr.de (P. Steigenberger), carey.noll@nasa.gov (C. Noll), frf@iss-reshetnev.ru (R. Fatkulin), kogure.satoshi@jaxa.jp (S. Kogure), asganesh@isac.gov.in (A.S. Ganeshan).

http://dx.doi.org/10.1016/j.asr.2015.06.019
0273-1177/

Knowledge of the spacecraft attitude is also important to account for the so-called phase wind-up effect (Wu et al., 1993), which describes the variation of the measured carrier-phase range with changes in the relative alignment of the receiver and transmitter antenna. Finally, the spacecraft attitude needs to be known when modeling solar radiation pressure, since the resulting acceleration depends directly on the orientation of the satellite body and the solar panels with respect to the incident radiation (Rodriguez-Solano et al., 2012).

Within the International GNSS Service (IGS; Dow et al., 2009), precise orbit and clock products for the United States' Global Positioning System (GPS) and the Russian Globalnaja Nawigazionnaja Sputnikowaja Sistema (GLONASS) are routinely generated as a basis for a wide range of scientific and engineering applications. For proper use of these products, a consistent description of the spacecraft geometry and attitude is required. Concerning the modeling of satellite antenna PCOs and PCVs, consistency between product generation and application is commonly achieved through standardized values for the antenna parameters (provided in IGS models in the antenna exchange format ANTEX; Rothacher and Schmid, 2010) and the assumption of a nominal body orientation outside the eclipse region. However, a clear attitude definition and reference are likewise critical for phase wind-up corrections when aiming at single-receiver ambiguity fixing in precise point positioning (Teunissen and Khodabandeh, 2015).

In case of GPS and GLONASS, standardization within the IGS has largely been facilitated through the fact that the individual satellites employ similar attitude control laws and enable a uniform description after aligning the designation of the principal spacecraft axes. With the advent of new GNSSs, a wider range of attitude control laws arises and a variety of manufacturer-specific conventions for the individual spacecraft coordinate systems has to be handled. As part of its Multi-GNSS Experiment (MGEX; Montenbruck et al., 2014), the IGS already provides early data products for many of the new constellations (including the European Galileo system, the Chinese BeiDou Navigation Satellite System, and the Japanese Quasi-Zenith Satellite System QZSS). Therefore, a need for a uniform and traceable description of the nominal spacecraft attitude as well as the GNSS antenna and SLR retroreflector coordinates has emerged.

In response to this need, the present article provides a description and mathematical formulation of GNSS attitude control laws for all satellite navigation systems currently in operation or under construction. It covers GPS, GLONASS, BeiDou, Galileo, QZSS, and the Indian Regional Navigation Satellite System (IRNSS), but excludes satellite-based augmentation systems (SBASs), which are not currently used for precise positioning applications. Also, the presentation is limited to normal operations and excludes eclipse transits, which require special attention (see, e.g., Kouba, 2009; Dilssner et al., 2011). Following a general introduction to the basic reference frames and the mathematical description of GNSS satellite orientation in space, definitions of the manufacturer- and IGS-specific spacecraft body frames are provided. For each constellation and all individual types ("blocks") of satellites, the alignment and naming of the principal spacecraft axes is documented through images, which enable a unique identification in relation to the spacecraft structure. Finally, GNSS antenna phase center coordinates and, where applicable, LRA coordinates of the various GNSS satellites are compiled for both the manufacturer- and the IGS-specific axis convention.

2. Reference frames

The various constellations of navigation satellites have different configurations and orbits. While medium-altitude Earth orbits (MEO) are used for Global Navigation Satellite Systems, geosynchronous orbits are employed to achieve a regional coverage. These geosynchronous orbits are commonly divided into inclined geosynchronous orbits (IGSO) and geostationary orbits (GEO) with an insignificant inclination. Table 1 provides an overview of the orbital characteristics and the different attitude modes employed by present satellite navigation systems.

The inertial attitude of a GNSS satellite is mostly determined by the need to point the navigation antenna toward the Earth, while keeping the solar panels oriented to the Sun. To achieve this goal, the spacecraft performs a continuous rotation about the Earth-pointing ("yaw") axis such as to keep the solar panel axis perpendicular to the Sun direction (Bar-Sever, 1996; Kouba, 2009). This concept, which was first implemented by the GPS and later adopted by most other constellations, is commonly known as *yaw-steering* (YS) attitude mode. As a disadvantage, this mode requires rapid yaw-slews of up to 180°, whenever the Sun is close to the orbital plane. In the latter case, an *orbit-normal* (ON) mode is often favored, in which the spacecraft body is fixed in the local orbital frame and the solar panel rotation axis is kept perpendicular to the orbital plane. In some cases, both attitude modes may be employed on the same satellite (Table 1), depending on

Table 1
General characteristics of GNSS orbits and attitude modes (i: inclination, T: orbital period, YS: yaw-steering, ON: orbit-normal).

Constellation	Type	i	T	Attitude
GPS		55°	11^h58^m	YS
GLONASS		65°	11^h16^m	YS
Galileo		56°	14^h05^m	YS
BeiDou-2	MEO	55°	12^h53^m	YS, ON (near-zero β)
	IGSO	55°	23^h56^m	YS, ON (near-zero β)
	GEO	≈0°	23^h56^m	ON
QZSS		43°	23^h56^m	YS, ON (low β)
IRNSS	IGSO	29°	23^h56^m	Biased YS
	GEO	≈0°	23^h56^m	Biased YS

the angle between the Sun and the orbital plane (usually denoted as β).

For a concise description of the different attitude laws, the relevant reference frames and their mutual relation are described in the subsequent paragraphs.

2.1. Body-fixed frame

To describe the orientation of a satellite in space, a body-fixed reference frame $\mathcal{R}_{\mathrm{BF}}$ needs to be defined. This frame is permanently tied to the mechanical structure of the satellite and enables the specification of antenna and LRA coordinates relative to the CoM. The body-fixed frame is likewise required to describe the position and alignment of individual surface elements for radiation pressure and thermal emission models (Feltens, 1991). The principal axes (i.e., the symmetry axes and/or the main axes of inertia) of the spacecraft body provide the natural choice for the definition of the body-fixed frame. The z_{BF}-axis is commonly aligned with the boresight direction of the GNSS antenna, while the rotation axis of the solar panels marks the $\pm y_{\mathrm{BF}}$-axis. However, no unique convention for the labeling of individual spacecraft axes exists. Instead, distinct frame orientations have been adopted for the various constellations and types of spacecraft depending on the manufacturer's heritage and preference.

To avoid a multitude of attitude descriptions differing only by a permutation of axes, the IGS has adopted a common body-fixed reference frame, $\mathcal{R}_{\mathrm{BF,IGS}}$, starting with the Block IIR GPS satellites and the early work on GLONASS. The axes of the $\mathcal{R}_{\mathrm{BF,IGS}}$ frame are strictly parallel (or antiparallel) to those of the manufacturer-specific $\mathcal{R}_{\mathrm{BF}}$ frame and likewise form a right-handed, orthonormal basis. However, the specific choice and sign of the individual axes enables a consistent description of the yaw-steering attitude across different constellations and spacecraft platforms within a constellation:

- The $+z_{\mathrm{BF,IGS}}$-axis is the principal body axis closest to the antenna boresight direction (i.e., the direction of the maximum beam intensity).
- The $y_{\mathrm{BF,IGS}}$-axis is parallel to the rotation axis of the solar panels. The positive $y_{\mathrm{BF,IGS}}$-direction is defined through the corresponding $x_{\mathrm{BF,IGS}}$-axis orientation.
- The $+x_{\mathrm{BF,IGS}}$-direction is chosen such that the $+x_{\mathrm{IGS}}$-panel is permanently sunlit during nominal yaw-steering, while the $-x_{\mathrm{IGS}}$-panel remains dark at all times.

This convention is based on the original spacecraft body frame assignment for the GPS Block II/IIA satellites (where $\mathcal{R}_{\mathrm{BF}} = \mathcal{R}_{\mathrm{BF,IGS}}$). For various other spacecraft (e.g., GPS Block IIR and Galileo), the two frames are related to each other by a sign change in the x- and y-axes or a more complicated permutation of the individual axes (e.g., GLONASS and IRNSS).

Even though the motivation of the $\mathcal{R}_{\mathrm{BF,IGS}}$ frame and the description given above are related to the *nominal* orientation of GNSS satellites relative to the Earth and Sun, it must be kept in mind that this frame is strictly body-fixed. In fact, its definition is *not* related to the actual spacecraft attitude, and the individual axes are always assigned relative to the spacecraft structure. For a concise and unambiguous specification, Section 3 provides distinct drawings for each individual spacecraft platform showing the orientation of both the manufacturer-specific and the IGS-specific body frame. It also provides a verbal description of the axis orientation based on the location of specific structural elements.

2.2. Antenna frame

Besides the body-fixed spacecraft frame discussed above, a dedicated antenna frame $\mathcal{R}_{\mathrm{ANT}}$ is required to describe PCOs, PCVs, or gain patterns of a stand-alone GNSS transmit antenna (e.g., derived from field or chamber calibrations; Mader and Czopek, 2001; Wübbena et al., 2007; Marquis, 2014b) and to describe the orientation of an antenna structure relative to the satellite body after assembly.

Unfortunately, information on manufacturer-specific axis conventions of GNSS antenna panels as well as assembly information are hardly available to the scientific community. So far, no explicit distinction has therefore been made by the IGS between the antenna frame and the spacecraft body frame of any GNSS satellite. This is essentially equivalent to the use of an IGS-specific antenna frame ($\mathcal{R}_{\mathrm{ANT,IGS}}$), oriented parallel to the axes of the IGS-specific spacecraft body frame: $\mathcal{R}_{\mathrm{ANT,IGS}} = \mathcal{R}_{\mathrm{BF,IGS}}$.

While the two frames can be considered as identical for most practical purposes, it is still important, though, to distinguish them conceptually. Ideally, antenna-related information should always be related to the native antenna frame and thus be decoupled from the actual mounting orientation on the host vehicle.

2.3. Local orbital frame

The local orbital frame $\mathcal{R}_{\mathrm{RTN}}$ is defined by the radial (R), along-track (T) and cross-track (N) directions and provides a natural reference for describing the attitude of an Earth pointing spacecraft. For a given satellite position $\boldsymbol{r}$ relative to the center of the Earth and an inertial velocity $\boldsymbol{v}$, the corresponding unit vectors are obtained as

$$\begin{aligned} \boldsymbol{e}_{\mathrm{R}} &= \frac{\boldsymbol{r}}{|\boldsymbol{r}|} \\ \boldsymbol{e}_{\mathrm{T}} &= \boldsymbol{e}_{\mathrm{N}} \times \boldsymbol{e}_{\mathrm{R}} \\ \boldsymbol{e}_{\mathrm{N}} &= \frac{\boldsymbol{r} \times \boldsymbol{v}}{|\boldsymbol{r} \times \boldsymbol{v}|}. \end{aligned} \tag{1}$$

The transformation

$$\boldsymbol{x}_{\mathrm{BF}} = \boldsymbol{A}_{\mathrm{BF}}^{\mathrm{RTN}} \cdot \boldsymbol{x}_{\mathrm{RTN}} \quad \text{and} \quad \boldsymbol{x}_{\mathrm{RTN}} = \left(\boldsymbol{A}_{\mathrm{BF}}^{\mathrm{RTN}}\right)^{\top} \cdot \boldsymbol{x}_{\mathrm{BF}} \tag{2}$$

between the orbital frame and the body-fixed frame is commonly described by a series of three elementary rotations

$$\boldsymbol{A}_{\mathrm{BF}}^{\mathrm{RTN}} = \boldsymbol{R}_x(\phi)\cdot\boldsymbol{R}_y(\vartheta)\cdot\boldsymbol{R}_z(\psi) \tag{3}$$

about the z-, y-, and x-axes by the angles ψ (yaw), ϑ (pitch), and ϕ (roll).

Considering the case of a nadir-pointing satellite (which naturally applies for GNSS satellites with only few exceptions), the pitch and roll angles vanish and the spacecraft attitude can be fully described by the yaw-angle alone. As illustrated in Fig. 1, the yaw-angle ψ specifies the angle between the $\boldsymbol{e}_{\mathrm{T}}$ and $\boldsymbol{e}_{x,\mathrm{BF}}$ vectors for a right-handed rotation about the $+z_{\mathrm{BF,IGS}}$- (or $-$R-) axis. For $\psi = 0°$, the spacecraft $+x_{\mathrm{BF}}$-axis is aligned with the transverse direction and $+y_{\mathrm{BF}}$ is oriented antiparallel to the orbital angular momentum.

2.4. Yaw-steering frame

The yaw-steering frame $\mathcal{R}_{\mathrm{YS}}$ defines the reference orientation for a nadir-pointing GNSS satellite with Sun-oriented solar panels. It is defined by the three unit vectors

$$\begin{aligned}\boldsymbol{e}_{x,\mathrm{YS}} &= \boldsymbol{e}_{y,\mathrm{YS}}\times\boldsymbol{e}_{z,\mathrm{YS}}\\ \boldsymbol{e}_{y,\mathrm{YS}} &= \frac{\boldsymbol{e}_\odot\times\boldsymbol{r}}{|\boldsymbol{e}_\odot\times\boldsymbol{r}|}\\ \boldsymbol{e}_{z,\mathrm{YS}} &= -\frac{\boldsymbol{r}}{|\boldsymbol{r}|},\end{aligned} \tag{4}$$

where $\boldsymbol{e}_\odot$ is a unit vector pointing from the satellite to the Sun. The vector $\boldsymbol{e}_{z,\mathrm{YS}}$ points toward the center of the Earth and $\boldsymbol{e}_{y,\mathrm{YS}}$ is perpendicular to the Sun and nadir directions. The above definitions imply that $\boldsymbol{e}_\odot\cdot\boldsymbol{e}_{x,\mathrm{YS}} > 0$, i.e., the unit vector in Sun direction and the $+x$-axis of the $\mathcal{R}_{\mathrm{YS}}$ frame are always part of the same hemisphere.

It may be noted that the frame orientation depends only on the Sun-spacecraft-Earth geometry but not on the instantaneous velocity or orbital plane. If the Sun is exactly in the radial direction, this frame is undetermined.

Except for a possible permutation of the axes, the body frame $\mathcal{R}_{\mathrm{BF}}$ of a spacecraft in nominal yaw-steering mode is continuously aligned with the $\mathcal{R}_{\mathrm{YS}}$ frame (see Fig. 2). For a given elevation β of the Sun above the orbit plane and an orbit angle μ (measured relative to the midnight point), the nominal yaw-angle is given by

$$\psi_{\mathrm{IGS}} = \mathrm{atan2}(-\tan\beta, \sin\mu) \tag{5}$$

when applying the IGS convention for the spacecraft body axes (Bar-Sever, 1996).

Even though the yaw-steering frame describes the nominal orientation of the body axes for many GNSS satellites, it is defined exclusively by the Sun-spacecraft-Earth geometry. As such, it must not be confused with a body-fixed frame and cannot be used for the specification of antenna coordinates.

2.5. Orbit-normal frame

The orbit-normal frame $\mathcal{R}_{\mathrm{ON}}$ defines the reference orientation of a spacecraft aligned with the orbital frame. Its axes are parallel (or antiparallel) to those of the local orbital frame discussed in Section 2.3, but the naming and direction of individual axes is chosen to match those of the body-fixed frame for a spacecraft in nominal orbit-normal mode. Accordingly, the z_{ON}-axis points to the center of the Earth and the y_{ON}-axis is perpendicular to the orbital plane. Two subcases may be defined, where the x_{ON}-axis is toward the velocity ($\mathcal{R}_{\mathrm{ON}^+}$ frame) or opposite to the velocity ($\mathcal{R}_{\mathrm{ON}^-}$ frame). The complete expressions are

$$\begin{aligned}\boldsymbol{e}_{x,\mathrm{ON}^+} &= +\boldsymbol{e}_{\mathrm{T}}\\ \boldsymbol{e}_{y,\mathrm{ON}^+} &= -\boldsymbol{e}_{\mathrm{N}}\\ \boldsymbol{e}_{z,\mathrm{ON}^+} &= -\boldsymbol{e}_{\mathrm{R}}\end{aligned} \tag{6}$$

and

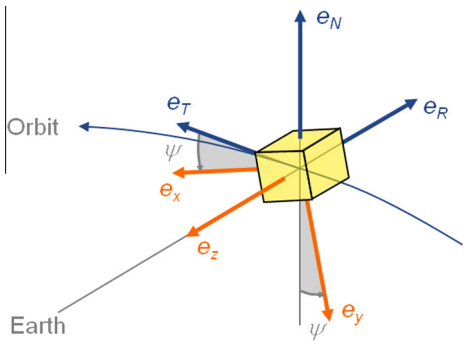

Fig. 1. Definition of the yaw-angle ψ for an Earth pointing spacecraft.

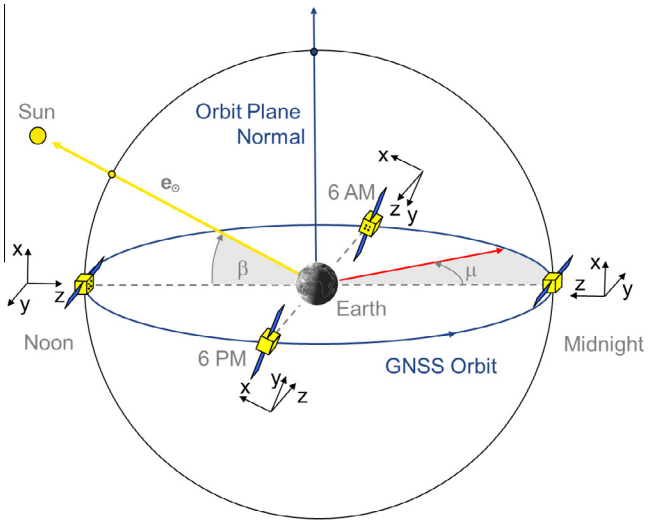

Fig. 2. GNSS satellite orientation in nominal yaw-steering mode. The x-, y- and z-vectors indicate the axes of the body-fixed reference frame $\mathcal{R}_{\mathrm{BF,IGS}}$ (following the IGS axis convention), which is here aligned with the $\mathcal{R}_{\mathrm{YS}}$ frame.

$$\begin{aligned} \boldsymbol{e}_{x,\mathrm{ON}^-} &= -\boldsymbol{e}_{\mathrm{T}} \\ \boldsymbol{e}_{y,\mathrm{ON}^-} &= +\boldsymbol{e}_{\mathrm{N}} \\ \boldsymbol{e}_{z,\mathrm{ON}^-} &= -\boldsymbol{e}_{\mathrm{R}}. \end{aligned} \tag{7}$$

The orientation of a spacecraft in orbit-normal mode and the corresponding pointing of its solar panels are shown in Fig. 3. It illustrates the case of a body frame aligned with the $\mathcal{R}_{\mathrm{ON}^+}$ frame, in which the x_{BF}-axis points in flight direction thus yielding a zero yaw-angle. The solar panel rotation angle (i.e., the angle between the solar panel normal and the z_{BF}-axis of the spacecraft body) matches the orbit angle μ, and the panels perform a full 360° turn throughout the orbit.

For a spacecraft aligned with the $\mathcal{R}_{\mathrm{ON}^-}$ frame, the orientation of the x_{BF}- and y_{BF}-axes is inverted with respect to Fig. 3 and the yaw-angle attains a value of $\psi = 180°$ at all times.

3. Satellite configurations and attitude modes

This section discusses the orientation of the body-fixed reference frames and the attitude modes for the individual GNSS constellations and spacecraft types.

3.1. GPS

The Global Positioning System is the first and oldest satellite navigation system in place today. Over more than 30 years, a variety of different spacecraft types, commonly termed as "Blocks" have been employed.

The first generation of GPS satellites ("Block I") was built by Rockwell International (Fruehauf, 2014). A total of 11 Block I spacecraft were launched between 1978 and 1985 (including the failed launch of space vehicle number

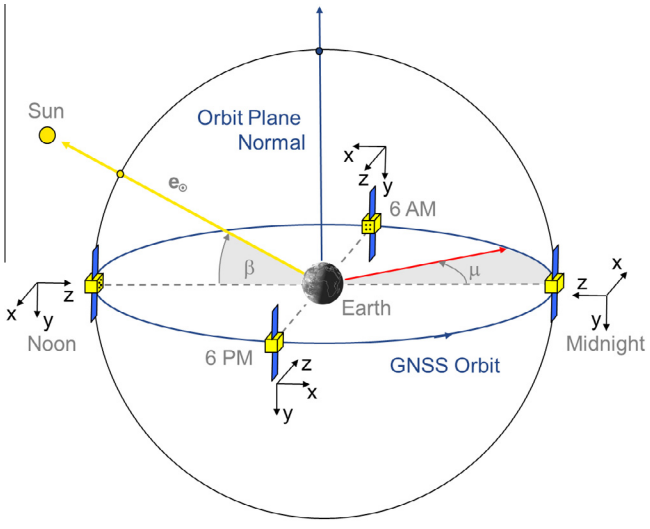

Fig. 3. GNSS satellite orientation in orbit-normal mode with a fixed yaw-angle of $\psi = 0°$. The x-, y- and z-vectors indicate the axes of the body-fixed reference frame $\mathcal{R}_{\mathrm{BF,IGS}}$ (following the IGS axis convention), which is here aligned with the $\mathcal{R}_{\mathrm{ON}^+}$ frame.

SVN 7), and the last satellite of this series was decommissioned in 1995 (Dorsey et al., 2006). The orientation of the body frame for the Block I satellites ($\mathcal{R}_{\mathrm{BF}} = \mathcal{R}_{\mathrm{BF,IGS}}$) as defined by Rockwell International (1974) is illustrated in Fig. 4. The figure shows one of the first 5 satellites of this series (SVN 1–5), which may be distinguished by the centered position of the GNSS antenna on the front panel. In subsequent units (SVN 6–11) the antenna was shifted in $+x$-direction to accommodate an additional Nuclear Detection (NUDET) payload. For both subtypes of the Block I spacecraft, the direction of the x- and y-axes can be uniquely identified by the location of the S-band telemetry and command antenna near the $+y$-side of the front panel. Note, however, that an inconsistent set of axis labels is used, e.g., by Fliegel et al. (1992).

The next generation of satellites (including the original Block II spacecraft and the slightly improved and more massive IIA satellites) was again built by the same prime contractor. As of early 2015, 3–5 Block IIA spacecraft remain in operational use, but are about to be replaced by the new GPS IIF and III satellites within 1–2 years. It may be noted that two Block IIA satellites (SVN 35 and 36) were equipped with LRAs. However, the satellites were decommissioned in 2014 and are no longer tracked by the International Laser Ranging Service (ILRS; Pearlman et al., 2002). The body-fixed reference frame of the Block II/IIA satellites is described in design drawings reproduced in Degnan and Pavlis (1994). As illustrated in Fig. 4, the positive z-axis is parallel to the boresight direction of the navigation antenna, and the y-axis coincides with the rotation axis of the solar panels. The x-axis is parallel to the long side of the front panel and the positive direction can be identified from the location of the navigation antenna and the LRA, both of which are offset in $+x$-direction from the CoM. Also, the $-x/-y$-corner can be easily identified by the large "horn" that serves as Sun shade for the optical burst detector of the NUDET payload. Similar to the Block I spacecraft, the IGS-specific body frame $\mathcal{R}_{\mathrm{BF,IGS}}$ matches the manufacturer-specific frame $\mathcal{R}_{\mathrm{BF}}$ for the Block II/IIA satellites.

Except for a small intentional yaw-bias of about 0.5°, the Block II/IIA satellites employ a yaw-steering attitude, in which the body frame is closely aligned with the yaw-steering frame specified in Eq. (4) during normal operations (i.e., $\mathcal{R}_{\mathrm{BF}} = \mathcal{R}_{\mathrm{BF,IGS}} \approx \mathcal{R}_{\mathrm{YS}}$; Bar-Sever, 1996). A special attitude control law applies for eclipse transits and the corresponding "noon turns" (Bar-Sever, 1996).

A different manufacturer, Lockheed Martin, was awarded the contract to build the Block IIR ("replenishment") satellites, which were put into operation starting in 1997. An enhanced version, known as Block IIR-M ("modernized") and launched between 2005 and 2009, first offered the new civil L2C signal and the new military M-code signals (Dorsey et al., 2006). These satellites make use of a modernized antenna panel (Marquis and Reigh, 2005) that was also employed for the final batch of classic

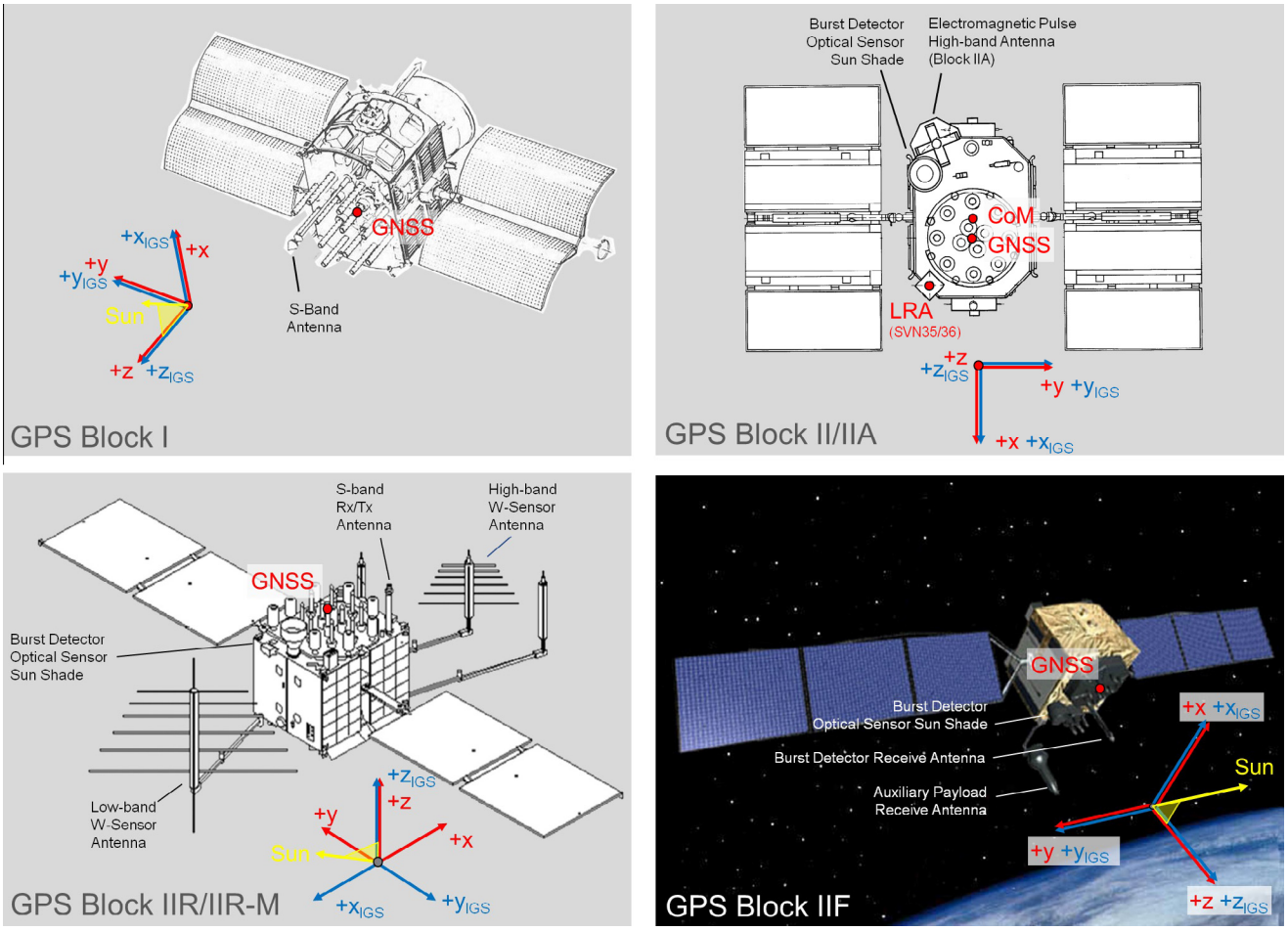

Fig. 4. Orientation of the spacecraft body frame for GPS Block I, II/IIA, IIR/IIR-M and IIF satellites. Red arrows and labels refer to the manufacturer-specific system $(x,y,z)_{\mathrm{BF}}$, while IGS axis conventions $(x,y,z)_{\mathrm{BF,IGS}}$ are shown in blue. For ease of notation, the index "$_{\mathrm{BF}}$" has been dropped in all axis labels. Red dots indicate the locations of the center-of-mass (CoM), the navigation antenna (GNSS), and the laser retroreflector array (LRA). Image credits and sources: Block I: Rockwell International; Block II/IIA: GPS World; Block IIR: ©2015 Lockheed Martin Corporation, all rights reserved, published with permission; Block IIF: Nat. Coord. Office for Space-Based PNT. (For interpretation of the references to color in this figure legend, the reader is referred to the web version of this article.)

Block IIR satellites (Dorsey et al., 2006). Due to different phase center locations, it is therefore common to distinguish a total of three subtypes (IIR-A, IIR-B, and IIR-M) of this spacecraft generation (Schmid et al., 2007).

The body-fixed coordinate system of the IIR satellites is shown in Fig. 4 based on design drawings contained in Marquis (2014b). As for all GPS satellites, the $+z_{\mathrm{BF}}$-axis is parallel to the antenna boresight direction and the $\pm y_{\mathrm{BF}}$-axis is aligned with the solar panel rotation axis. The positive x_{BF}-axis points from the low-band W-sensor antenna (large "Christmas tree") to the high-band counterpart (small "Christmas tree"). Other clearly distinguishable features, which are useful to identify the axis orientation, include the Sun shade of the optical burst detector (on the $-x_{\mathrm{BF}}$-side of the front panel) and the S-band antenna (in the $+x_{\mathrm{BF}}/-y_{\mathrm{BF}}$-corner). Similar to their predecessors, the Block IIR satellites employ a yaw-steering attitude but keep the $-x_{\mathrm{BF}}$-face pointing toward the Sun (Bar-Sever, 1997; Marquis, 2014a). Accordingly, the x- and y-axes of the IGS-specific body frame $\mathcal{R}_{\mathrm{BF,IGS}}$ are inverted with respect to those of the manufacturer-specific $\mathcal{R}_{\mathrm{BF}}$ frame. While the Block IIR spacecraft orientation is usually aligned with the yaw-steering frame, exceptions apply for the attitude control during noon and midnight turns in the eclipse season. These are beyond the scope of the present work, and readers are referred to Kouba (2009) for further details.

For completeness, we note that the IIR satellites may also employ an orbit-normal mode in which the spacecraft is aligned with the orbital frame ($\mathcal{R}_{\mathrm{BF}} = \mathcal{R}_{\mathrm{ON}^+}$, $\mathcal{R}_{\mathrm{BF,IGS}} = \mathcal{R}_{\mathrm{ON}^-}$):

> "For beta angles between 1.6 deg and −1.6 deg, the satellite switches to a fixed yaw mode. This transition happens at orbit dusk. During this mode the X and Z axes are in the orbital plane, where +X points roughly in the direction of velocity" (Bar-Sever, 1997).

However, this low-beta mode has been discontinued and is no longer in use according to Marquis and Krier (2000) and Kouba (2009).

The latest generation of GPS satellites, termed IIF for "follow-on" is built by Boeing. Between 2010 and spring 2015, a total of nine Block IIF satellites has been added to the GPS constellation. The orientation of the spacecraft coordinate system is shown in Fig. 4 based on design drawings contained in Fisher and Ghassemi (1999) and Dorsey et al. (2006). The direction of the positive x-axis can most easily be identified from the placement of the large auxiliary payload receive antenna, which extends from the $-x$-face. Furthermore, a $+x$-offset of the navigation antenna relative to the center of the Earth-facing $+z$-panel may be recognized. The manufacturer-specific axis designation is compatible with the IGS convention, as indicated by the (positive) x-offset of the antenna derived by Dilssner (2010), who adopted an IGS-style yaw-steering attitude for the PCO and PCV estimation of the IIF spacecraft. Specific aspects of the IIF attitude control law during the eclipse season are likewise discussed in Dilssner (2010).

3.2. GLONASS

The Russian GLONASS has, so far, employed three different types of spacecraft. These were developed by the governmental "Academician Reshetnev Research & Production Association of Applied Mechanics (NPO PM)", which later became the Joint Stock Company "Information Satellite Systems (ISS) – Reshetnev Company".

The deployment of the GLONASS constellation was started with the launch of a first-generation GLONASS satellite (Fig. 5) in October 1982 (Johnson, 1994; Langley, 1997). A total of 99 GLONASS satellites were launched between 1982 and 2005, and the last satellite (No. 795) of this series was decommissioned in August 2009. The GLONASS satellites transmitted Frequency Division Multiple Access (FDMA) navigation signals on the L1 and L2 carrier frequencies through the phased-array navigation antenna.

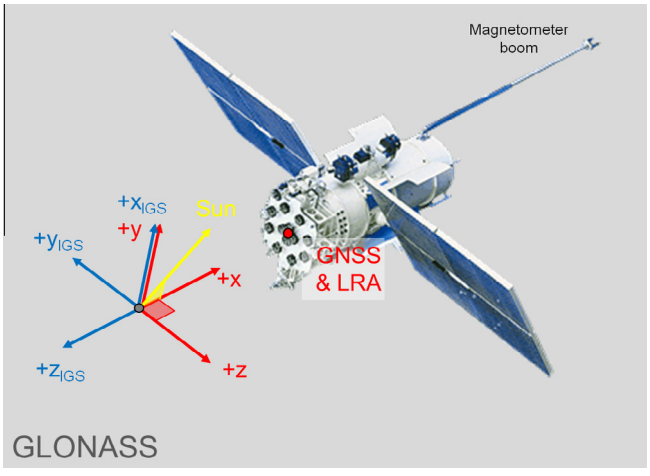

Fig. 5. Orientation of the spacecraft body frame for the first-generation GLONASS satellites. Red arrows and labels refer to the manufacturer-specific system, while IGS axis conventions are shown in blue. Image Credits: ISS-Reshetnev. (For interpretation of the references to color in this figure legend, the reader is referred to the web version of this article.)

The present constellation consists mostly of GLONASS-M satellites (Fig. 6). These were first launched in 2003, and a total of 42 satellites of this series were launched up to the end of 2014. Like its predecessor, the construction of the GLONASS-M spacecraft is based on a pressurized container, which forms the cylindrical main body of the satellite. The main part of the on-board equipment is accommodated on a structural frame inside this container. To provide the required temperature, the container is shaded using folds (louvers) which are periodically opened and closed by means of a drive motor. Depending on the current temperature inside the container, the opening and closing of the folds provides a corresponding increase or decrease of the radiation surface.

GLONASS-M satellites transmit FDMA navigation signals on the L1 and L2 carrier frequencies through the phased-array navigation antenna. The last seven satellites of this series (No. 755–761) were improved to allow transmission of the new Code Division Multiple Access (CDMA) signal on the L3 carrier frequency using a separate navigation antenna. A diversity of experiments was conducted on-board GLONASS-M satellites. The main purpose of these experiments was to space-qualify advanced equipment for next-generation satellites and to check technologies different from those used earlier. The experimental equipment was mainly accommodated outside the sealed container on the shady $+y_{BF}$-side.

A key difference of the follow-on GLONASS-K1 satellites (Fig. 6) and the future GLONASS-K2 satellites from previous satellite generations is the introduction of an unsealed satellite body based on honeycomb panels. It accommodates the on-board equipment and provides the corresponding thermal environment. The $\pm z_{BF}$ honeycomb panels are negligibly Sun-illuminated and the $+y_{BF}$-panel is located on the shady side of the satellite. Therefore, these panels are used to hold the main part of the heat dissipating equipment.

Another new feature of the GLONASS-K satellites is the provision of a COSPAS-SARSAT (Cosmicheskaya Sistema Poiska Avariynyh Sudov – Search And Rescue Satellite-Aided Tracking; Ilcev, 2007) transponder. Like the latest GLONASS-M satellites, the GLONASS-K1 satellites transmit CDMA signals on the L3 frequency next to the FDMA signals on L1 and L2. A distinct L3 antenna is used on the first K1 satellite (No. 701), while an improved L1/L2/L3 phased-array navigation antenna is used from No. 702 onwards. The first GLONASS-K1 satellite was launched in February 2011. Nowadays (spring 2015), two satellites of this series are under flight tests.

Unlike GPS, all GLONASS satellites are equipped with LRAs to support SLR measurements for orbit validation.

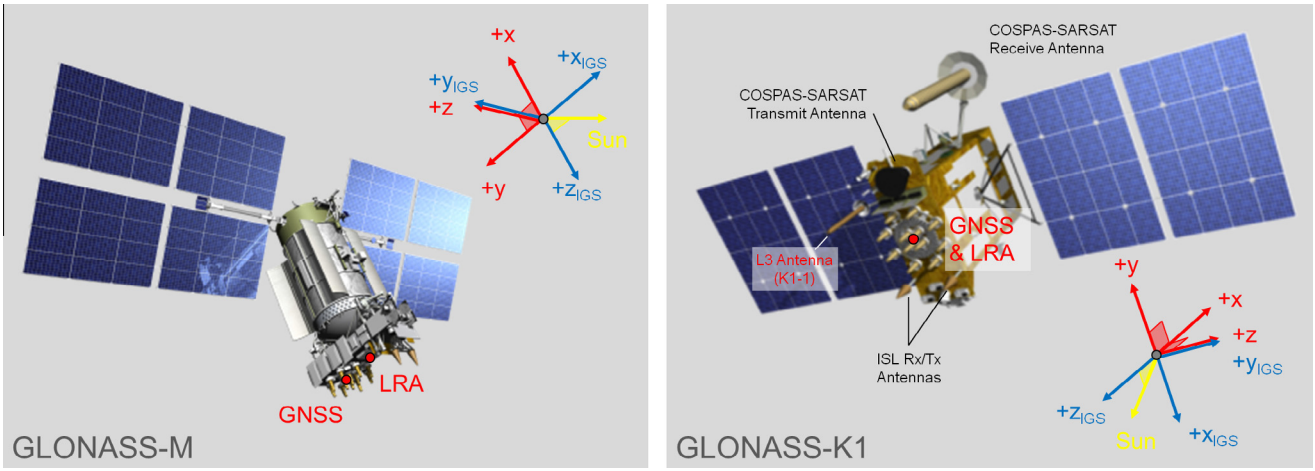

Fig. 6. Orientation of the spacecraft body frame for GLONASS-M and -K1 satellites. Red arrows and labels refer to the manufacturer-specific system, while IGS axis conventions are shown in blue. For GLONASS-K1, the antenna locations of the radio-based inter-satellite link (ISL) and the COSPAS-SARSAT distress alert system are labeled to assist the identification of the spacecraft axes. Image Credits: ISS-Reshetnev. (For interpretation of the references to color in this figure legend, the reader is referred to the web version of this article.)

The GLONASS satellites employ a nominal yaw-steering outside the eclipse period and special attitude control laws are applied for eclipse transits and the corresponding "noon turn". The aspects of these attitude control laws are described in Fateev et al. (2013, 2014). A nominal yaw-steering is also considered as standard model for the GLONASS orbit and clock determination outside eclipse periods within the IGS. For GLONASS-M satellites, a specific attitude model describing the yaw-angle variation near noon and midnight has been independently established by Dilssner et al. (2011) based on the analysis of GLONASS observations.

The manufacturer-specific spacecraft coordinate systems of the GLONASS, GLONASS-M, and GLONASS-K1 satellites are illustrated in Figs. 5 and 6. The $+x_{BF}$-axis of all spacecraft is oriented opposite to the antenna boresight direction, and the z_{BF}-axis coincides with the rotation axis of the solar panels. In case of the GLONASS-M, GLONASS-K1, and follow-on satellites, the $+y_{BF}$-axis is oriented in a direction away from the Sun during yaw-steering attitude control (Mitrikas, 2005, 2011). For consistency with IGS conventions, the following axis labeling is employed in the $\mathcal{R}_{BF,IGS}$ frame for these satellites:

$$\begin{aligned} +x_{BF,IGS} &= -y_{BF} \\ +y_{BF,IGS} &= +z_{BF} \\ +z_{BF,IGS} &= -x_{BF}. \end{aligned} \tag{8}$$

However, the orientation of the $+y_{BF}$-axis for the first-generation GLONASS satellites differs from the above. Here, the $+y_{BF}$-axis was oriented toward the Sun (Revnivykh and Mitrikas, 1998). Accordingly, the following axis labeling is employed in the $\mathcal{R}_{BF,IGS}$ frame for consistency with IGS conventions:

$$\begin{aligned} +x_{BF,IGS} &= +y_{BF} \\ +y_{BF,IGS} &= -z_{BF} \\ +z_{BF,IGS} &= -x_{BF}. \end{aligned} \tag{9}$$

In case of the GLONASS-M satellites, the orientation of the body frame can be recognized from the asymmetric location of the navigation antenna, which is shifted by about 0.5 m in $+y_{BF}$- ($-x_{BF,IGS}$-) direction relative to the geometric center of the Earth-facing panel. At the same time, the LRA exhibits a small offset of about 0.1 m in the opposite direction. For GLONASS and GLONASS-K1 satellites, in contrast, both the center of the antenna and the LRA are placed into the origin of the $+x_{BF,IGS}/+y_{BF,IGS}$-plane.

The axis orientation of the GLONASS-K1 satellites can best be verified through the COSPAS-SARSAT receive antenna, which is located outside the satellite body next to the $+z_{BF}/+y_{BF}$-edge. The transmit antenna for L3 CDMA signals shown in Fig. 6 was only used on-board GLONASS-K1 No. 701. Starting from No. 702, GLONASS-K1 satellites are equipped with an improved phased-array navigation antenna covering all three frequencies.

3.3. Galileo

The European Galileo system which is currently under construction has employed various types of spacecraft platforms throughout its evolution. As part of the Galileo In-Orbit Validation Element (GIOVE), two early test satellites called GIOVE-A and -B were launched in 2005 and 2008, respectively. These satellites served to secure the Galileo frequencies and to validate critical technology components. Following the successful launch and qualification of the first set of full-featured Galileo IOV (In-Orbit Validation) satellites, both GIOVE-A and -B were decommissioned in mid-2012. A total of four IOV satellites built by EADS Astrium was launched in 2011 and 2012. For the Full Operational Capability (FOC) phase of Galileo, a second generation of spacecraft was developed by OHB Systems. IOV and FOC satellites will jointly be part of the operational system.

As part of a MEO constellation, GIOVE-A (Johnston et al., 2008), GIOVE-B (Zentgraf et al., 2006), and the IOV satellites (Konrad et al., 2007) all use a yaw-steering attitude control strategy outside eclipse seasons. Although not publicly confirmed so far, it may be assumed that the same applies for the latest generation of FOC satellites. For GIOVE-B and the IOV satellites, a patented "dynamic yaw-steering" (Ebert and Oesterlin, 2008) is employed for β angles of less than 2°. In this case, the true β angle in the yaw-angle computation is replaced by a "smoothed" version to keep the maximum slew rate at noon and midnight within the design limits, while avoiding discontinuities in the yaw-rate and its higher-order derivatives.

The orientation of the manufacturer-specific spacecraft coordinate systems of GIOVE-A and -B is documented in Zandbergen and Navarro (2008) and can be inferred from publicly available LRA offset information (ILRS, 2015b) for the IOV and FOC spacecraft. Similar to GPS, the $+z_{BF}$- and $\pm y_{BF}$-axes are aligned with the antenna boresight direction and the solar panel rotation axis, respectively, but the $+x_{BF}$-panel is oriented away from the Sun during nominal yaw-steering. Therefore, the x- and y-axes of the IGS-specific $\mathcal{R}_{BF,IGS}$ body frame are inverted with respect to the manufacturer-specific frame for all types of Galileo satellites (Fig. 7).

3.4. BeiDou

Unlike the three navigation systems discussed so far, the Chinese second-generation BeiDou system employs a mixed constellation of MEO, IGSO and GEO satellites to achieve a regional and – in the future – global navigation service. All BeiDou-2 spacecraft are based on the DongFangHong-3 (DFH-3) platform (MEOs and IGSOs; Han et al., 2011) or the modified DFH-3A version

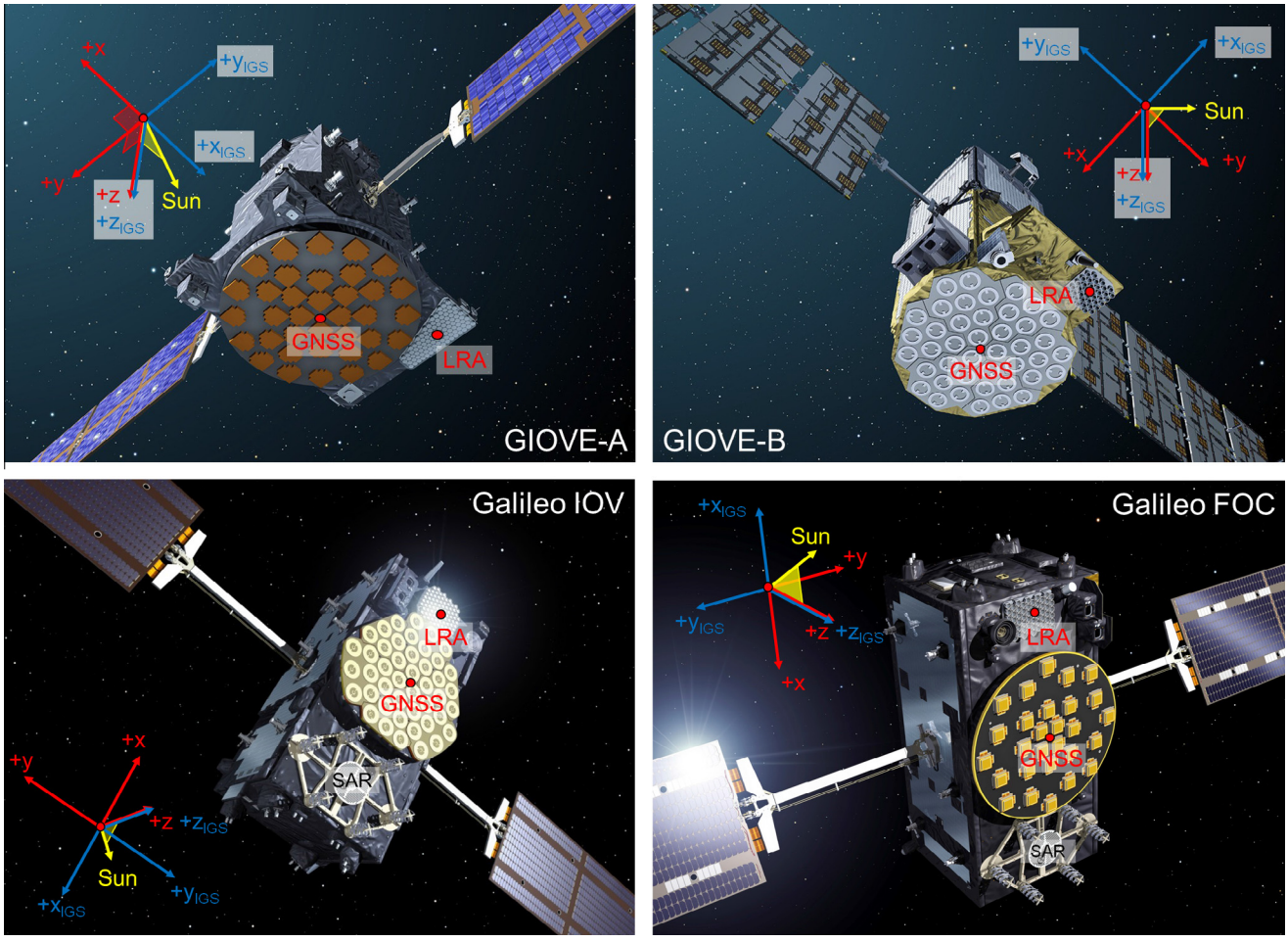

Fig. 7. Orientation of the spacecraft body frame for GIOVE-A/B and Galileo IOV/FOC satellites. Red arrows and labels refer to the manufacturer-specific system, while IGS axis conventions are shown in blue. Note that Sun illumination and solar panel alignment in the artist's drawings do not match the actual spacecraft orientation (except for the Galileo FOC image). During nominal yaw-steering, the Sun direction is confined to the $+x_{IGS}/\pm z_{IGS}$-half-plane as indicated by a representative Sun vector shown in yellow. For the Galileo IOV and FOC satellites, the location of the search-and-rescue (SAR) antenna is identified in addition to the GNSS antenna and LRA. Note, however, that the LRA and SAR antenna placement with respect to the spacecraft $+x$-axis is inverted for the two types of spacecraft. Image credits: ESA. (For interpretation of the references to color in this figure legend, the reader is referred to the web version of this article.)

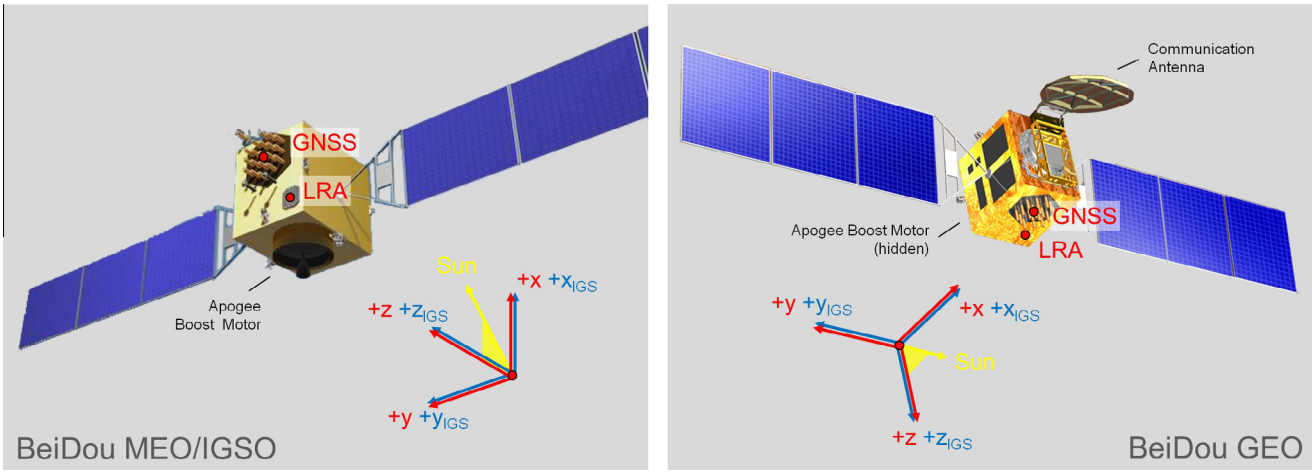

Fig. 8. Orientation of the spacecraft body frame for BeiDou MEO/IGSO and GEO satellites. Red arrows and labels refer to the manufacturer-specific system, while IGS axis conventions are shown in blue. During nominal yaw-steering, the Sun direction is confined to the $+x_{IGS}/\pm z_{IGS}$-half-plane as indicated by a representative Sun vector shown in yellow. Image credits: CSNO. (For interpretation of the references to color in this figure legend, the reader is referred to the web version of this article.)

(GEOs; Jun et al., 2012). In addition to the common payload elements, the GEO satellites carry a large communication antenna on the panel opposite to the apogee boost motor. Similar to GLONASS, all BeiDou satellites carry an LRA to support SLR tracking.

The spacecraft coordinate system as inferred from published coordinates of the LRA is illustrated in Fig. 8. The $+z_{BF}$-axis is aligned with the antenna boresight, and the $\pm y_{BF}$-axis is parallel to the solar panel rotation axis. The orientation of the $+x_{BF}$-axis can be recognized from the location of the apogee boost motor ($-x_{BF}$-panel) and, for GEOs, the C-band antenna ($+x_{BF}$-panel). For all types of BeiDou-2 spacecraft, the GNSS antenna is offset in $+x_{BF}$-direction from the center of the front panel, while the LRA is accommodated in the $-x_{BF}/-y_{BF}$-corner.

According to Wang et al. (2013), the BeiDou-2 MEO and IGSO satellites use a nominal yaw-steering as long as the Sun elevation β above the orbital plane exceeds a certain threshold. In the yaw-steering mode, the $+x_{BF}$-panel is sunlit, which implies that the IGS-specific body frame matches the manufacturer-specific frame ($\mathcal{R}_{BF} = \mathcal{R}_{BF,IGS}$). For low β angles, an orbit-normal mode with a forward pointing $+x_{BF}$-axis is employed to avoid rapid noon and midnight slews (Wang et al., 2013). The orbit-normal attitude is continuously maintained by the GEO satellites of the BeiDou constellation (Zhou et al., 2013). Based on the similarity of BeiDou MEO/IGSO and GEO spacecraft, the orientation of the IGS-specific body frame is likewise chosen to match the manufacturer-specific frame for the GEO spacecraft ($\mathcal{R}_{BF} = \mathcal{R}_{BF,IGS}$). The yaw-angle ($\psi_{BF} = \psi_{BF,IGS}$) is therefore zero for all MEO/IGSO spacecraft in orbit-normal mode as well as for all GEO satellites of the BeiDou-2 constellation. According to analyses of Guo and Zhao (2014), the transition of the MEO/IGSO attitude control from YS- to ON-mode and vice versa takes place at a β angle threshold of about 4°.

3.5. QZSS

The Japanese QZSS currently operates a single satellite, called QZS-1 ("Michibiki"). The spacecraft acts as a prototype satellite demonstrating key technologies, but is not necessarily representative of the fully operational constellation currently under development.

Aside from the main antenna used to transmit navigation signals in the L1, L2, E6 and L5 bands, the QZS-1 spacecraft carries an auxiliary antenna for transmission of the so-called SAIF (Submeter-class Augmentation with Integrity Function) signal. Furthermore, the spacecraft is equipped with an LRA for SLR distance measurements. The body-fixed coordinate system as described by Kogure (2012) is illustrated in Fig. 9. The $+z_{BF}$-axis points

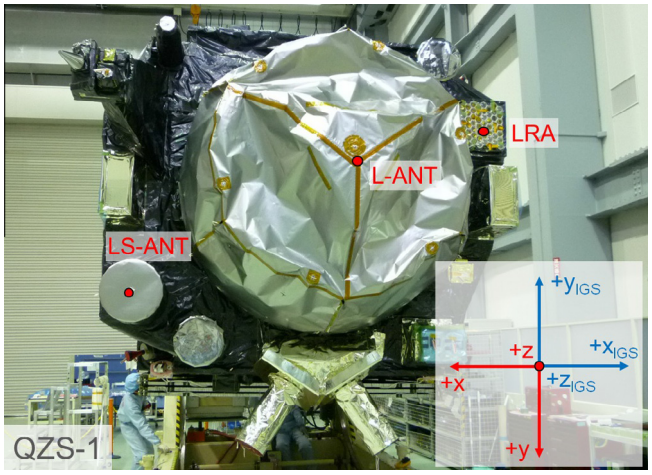

Fig. 9. Orientation of the spacecraft body frame for the first QZSS satellite. Red arrows and labels refer to the manufacturer-specific system, while IGS axis conventions are shown in blue. Red dots indicate the location of the main antenna (L-ANT), the SAIF antenna (LS-ANT) and the LRA. Image credits: JAXA/ILRS. (For interpretation of the references to color in this figure legend, the reader is referred to the web version of this article.)

in the antenna boresight direction, and the y_{BF}-axis coincides with the rotation axis of the solar panels. The SAIF antenna is mounted in the $+x_{BF}/+y_{BF}$-corner of the front panel, while the LRA is located in the opposite quadrant.

The attitude control system design and operational models of the QZS-1 spacecraft are described by Ishijima et al. (2009). For sufficiently large Sun elevations above the orbital plane (i.e., $|\beta| > 20°$), the satellite follows a nominal yaw-steering attitude with its $+x_{BF}$-axis pointing toward deep space (i.e., away from the Sun). Accordingly, the x- and y-axes of the IGS-specific $\mathcal{R}_{BF,IGS}$ body frame are inverted with respect to the manufacturer-specific $\mathcal{R}_{BF}$ frame.

Below the limiting β angle, the spacecraft follows an orbit-normal orientation with its $+x_{BF}$-axis oriented in forward direction and the $+y_{BF}$ solar panel pointing opposite to the orbital angular momentum ($\psi_{BF} = 0°$, $\mathcal{R}_{BF} = \mathcal{R}_{ON^+}$). This corresponds to an $\mathcal{R}_{ON^-}$ alignment of the IGS-specific body frame and an associated yaw-angle of $\psi_{BF,IGS} = 180°$. Based on a joint analysis of GNSS signals from the standard L-band antenna and the SAIF antenna, Hauschild et al. (2012) showed that the transition between YS- and ON-mode does not take place exactly at the nominal β angle threshold, but is typically performed at a convenient epoch nearby when the yaw-angle in YS- and ON-mode differ least.

3.6. IRNSS

The Indian Regional Navigation Satellite System (IRNSS) is conceived as a standalone navigation system for the Indian subcontinent and adjacent regions. In its final deployment stage, IRNSS will comprise three geostationary satellites and four geosynchronous satellites in moderately inclined orbits. All spacecraft make use of the INSAT-1000 (I-1K) satellite bus originally developed by the Indian Space Research Organization (ISRO) for small meteorological and communication satellites in geostationary orbit.

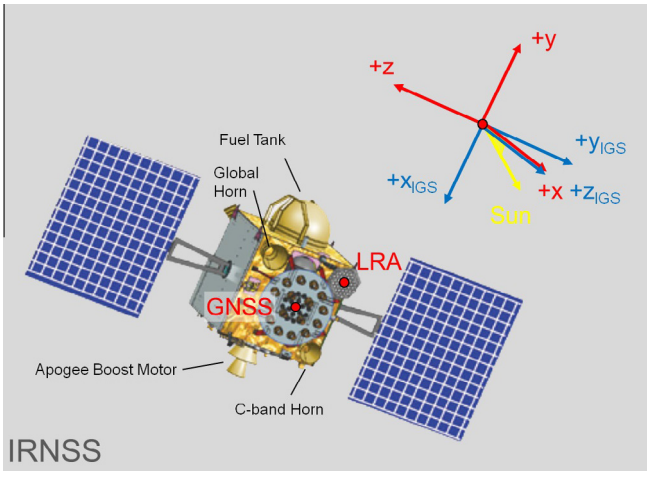

Fig. 10. Orientation of the spacecraft body frame for the IRNSS satellites. Red arrows and labels refer to the manufacturer-specific system, while IGS axis conventions are shown in blue. Image credits: ISRO. (For interpretation of the references to color in this figure legend, the reader is referred to the web version of this article.)

The manufacturer-specific coordinate system as described by Ganeshan (2014) is shown in Fig. 10. The $+x_{BF}$-axis coincides with the antenna boresight, the z_{BF}-axis is parallel to the solar panel rotation axis, and the $+y_{BF}$-axis (pointing from the apogee boost motor to the fuel tank) completes the right-handed system.

The IRNSS IGSO and GEO spacecraft both employ a yaw-steering attitude control with a sunlit $-y_{BF}$-panel (Ganeshan, 2014). Accordingly, the IGS-specific body frame is defined by the following axis assignment:

$$\begin{aligned} +x_{BF,IGS} &= -y_{BF} \\ +y_{BF,IGS} &= -z_{BF} \\ +z_{BF,IGS} &= +x_{BF}. \end{aligned} \tag{10}$$

It has to be kept in mind, though, that the orientation of the $\mathcal{R}_{BF,IGS}$ frame during nominal operations does not match the ideal yaw-steering frame $\mathcal{R}_{YS}$ as introduced in Section 2.4 even with this updated axis convention. As a unique feature, the IRNSS satellites continuously point the navigation antenna to a fixed point in the primary service area ($\lambda_0 = 83°$E, $\varphi_0 = 5°$N). This improves the available signal strength for IRNSS users but results in yaw, pitch, and roll offsets of several degrees compared to a nominal yaw-steering attitude.

Adopting, for simplicity, an Earth-fixed reference system and ignoring Earth oblateness, the target point of the navigation antenna beam is located at

$$\boldsymbol{r}_0 = \begin{pmatrix} \cos\varphi_0 \cos\lambda_0 \\ \cos\varphi_0 \sin\lambda_0 \\ \sin\varphi_0 \end{pmatrix} \tag{11}$$

In analogy with Eq. (4), the unit vectors of the IRNSS-specific nominal yaw-steering frame are then obtained as

$$\begin{aligned} \boldsymbol{e}_{x,\text{YS-IRNSS}} &= \boldsymbol{e}_{y,\text{YS-IRNSS}} \times \boldsymbol{e}_{z,\text{YS-IRNSS}} \\ \boldsymbol{e}_{y,\text{YS-IRNSS}} &= \frac{\boldsymbol{e}_\odot \times (\boldsymbol{r} - \boldsymbol{r}_0)}{|\boldsymbol{e}_\odot \times (\boldsymbol{r} - \boldsymbol{r}_0)|} \\ \boldsymbol{e}_{z,\text{YS-IRNSS}} &= -\frac{\boldsymbol{r} - \boldsymbol{r}_0}{|\boldsymbol{r} - \boldsymbol{r}_0|}. \end{aligned} \tag{12}$$

3.7. Simplified attitude laws for multi-GNSS processing

While the detailed modeling of GNSS satellite attitudes for precise orbit determination and point positioning requires a careful consideration of the system- and even spacecraft-specific control laws, a reasonable approximation for non-eclipse phases is given by the nominal yaw-steering or orbit-normal attitude.

By adopting the IGS-specific body frame orientation, the description for different constellations can, to a large extent, be unified (Table 2). The nominal yaw-steering

Table 2
Nominal attitude (orientation of the IGS-specific body frame) of individual navigation satellite types outside eclipse periods.

Constellation	Type	Attitude
GPS	I, II/IIA, IIR, IIF	$\mathcal{R}_{BF,IGS} = \mathcal{R}_{YS}$
GLONASS	–, M, K1	$\mathcal{R}_{BF,IGS} = \mathcal{R}_{YS}$
Galileo	GIOVE-A/B, IOV, FOC	$\mathcal{R}_{BF,IGS} = \mathcal{R}_{YS}$
BeiDou-2	MEO, IGSO	$\mathcal{R}_{BF,IGS} = \left\{ \begin{matrix} \mathcal{R}_{YS} \\ \mathcal{R}_{ON^+} \end{matrix} \right\}$ for $\lvert\beta\rvert \left\{ \begin{matrix} \geqslant \\ < \end{matrix} \right\} 4°$
	GEO	$\mathcal{R}_{BF,IGS} = \mathcal{R}_{ON^+}$
QZSS	QZS-1	$\mathcal{R}_{BF,IGS} = \left\{ \begin{matrix} \mathcal{R}_{YS} \\ \mathcal{R}_{ON^-} \end{matrix} \right\}$ for $\lvert\beta\rvert \left\{ \begin{matrix} \geqslant \\ < \end{matrix} \right\} 20°$
IRNSS	IGSO, GEO	$\mathcal{R}_{BF,IGS} = \mathcal{R}_{YS-IRNSS} \approx \mathcal{R}_{YS}$

Table 3
Offset of the navigation antenna phase center from the CoM for different Global and Regional Navigation Satellite Systems.

Constellation	Type	x [mm]	y [mm]	z [mm]	x_{IGS} [mm]	y_{IGS} [mm]	z_{IGS} [mm]	Comments
GPS	I	0.0	0.0	+1952.0	0.0	0.0	+1952.0	[a]
		+210.0	0.0	+1952.0	+210.0	0.0	+1952.0	[b]
	II/IIA	+279.0	0.0	+2564.0	+279.0	0.0	+2564.0	[c]
	IIR-A	0.0	0.0	+1308.0	0.0	0.0	+1308.0	[d]
	IIR-B/M	0.0	0.0	+847.0	0.0	0.0	+847.0	[d]
	IIF	+394.0	0.0	+1600.0	+394.0	0.0	+1600.0	[e]
GLONASS	–	−1840.1	0.0	0.0	0.0	0.0	+1840.1	[f]
	M	−2298.1	+545.0	0.0	−545.0	0.0	+2298.1	[f]
		−2067.0	+1100.0	0.0	−1100.0	0.0	+2067.0	[g]
	K1	−1760.1	0.0	0.0	0.0	0.0	+1760.1	[f]
		−1798.0	+620.0	−570.0	−620.0	−570.0	+1798.0	[h]
		−1426.0	0.0	0.0	0.0	0.0	+1426.0	[i]
Galileo	GIOVE-A	+4.0	−1.0	+862.0	−4.0	+1.0	+862.0	[j]
	GIOVE-B	+3.2	−3.4	+1351.7	−3.2	+3.4	+1351.7	[j]
	IOV	+200.0	0.0	+600.0	−200.0	0.0	+600.0	[k]
	FOC	−150.0	0.0	+1000.0	+150.0	0.0	+1000.0	[l]
BeiDou-2	MEO	+600.0	0.0	+1100.0	+600.0	0.0	+1100.0	[m]
	IGSO	+600.0	0.0	+1100.0	+600.0	0.0	+1100.0	[m]
	GEO	+600.0	0.0	+1100.0	+600.0	0.0	+1100.0	[m]
QZSS	QZS-1	+0.9	−2.9	+3197.9	−0.9	+2.9	+3197.9	[n]
		+1150.9	+697.1	+3015.1	−1150.9	−697.1	+3015.1	[o]
IRNSS	–	+1280.8	−11.4	−1.1	+11.4	+1.1	+1280.8	[p]

Notes:
[a] L1/L2 conventional values for the first lot (SVN 1–5) of Block I spacecraft with centered antenna panel.
[b] L1/L2; conventional (x, y; Zumberge, 1992), igs08.atx block mean (z); values apply for the second lot (SVN 6–11) of Block I spacecraft.
[c] L1/L2; conventional (x, y; Zumberge, 1992), igs08.atx block mean (z).
[d] L1/L2; conventional (x, y; Bar-Sever, 1997), igs08.atx block mean (z).
[e] L1/L2; conventional (x, y; Dilssner, 2010), preliminary mean (z; Schmid and Khachikyan, 2012).
[f] L1/L2 (measured; Fatkulin, 2015).
[g] L3 (measured; Fatkulin, 2015); values apply for GLONASS-M No. 755–761 with L3 payload.
[h] L3 (measured; Fatkulin, 2015); values apply for GLONASS-K1 No. 701.
[i] L3 (measured; Fatkulin, 2015); values apply for GLONASS-K1 No. 702 and follow-on K1 satellites.
[j] E1 (measured; Zandbergen and Navarro, 2008).
[k] E1, E5a/b/ab, E6 (conventional; Rizos et al., 2013).
[l] E1/E5a; conventional values for FOC-1/2 after orbit raising (rounded FOC-1 PCO estimate from Steigenberger et al., 2015). Different values may apply for follow-on FOC satellites.
[m] B1, B2, B3 (conventional; Rizos et al., 2013).
[n] L-ANT, L1 (measured; w.r.t. CoM 7/2012; Kogure, 2012).
[o] LS-ANT, L1 (measured; w.r.t. CoM 7/2012; Kogure, 2012).
[p] L5/S (measured; Ganeshan, 2015).

frame defined in Section 2.4 provides the reference orientation for the IGS body axes of all GPS, GLONASS, and Galileo satellites outside eclipse seasons and is likewise applicable for BeiDou MEO/IGSO satellites and QZS-1 at sufficiently large β angles. The well-established attitude description for the legacy GPS and GLONASS constellations can thus be utilized as well for many of the new navigation satellite systems. However, consideration of orbit-normal attitude modes with yaw-angles of both $\psi_{IGS} = 180°$ and $\psi_{IGS} = 0°$ is required in addition to the

Table 4
Offset of the LRA phase center from the CoM for different Global and Regional Navigation Satellite Systems.

Constellation	Type	x [mm]	y [mm]	z [mm]	x_{IGS} [mm]	y_{IGS} [mm]	z_{IGS} [mm]	Comments
GPS	IIA	+862.6	−524.5	+669.5	+862.6	−524.5	+669.5	[a]
GLONASS	–	−1554.7	0.0	0.0	0.0	0.0	+1554.7	[b]
	M	−1873.7	−137.0	+3.0	+137.0	+3.0	+1873.7	[c]
	K1	−1473.0	0.0	0.0	0.0	0.0	+1473.0	[d]
Galileo	GIOVE-A	−828.0	−655.0	+680.0	+828.0	+655.0	+680.0	[e]
	GIOVE-B	−804.3	+294.1	+1330.1	+804.3	−294.1	+1330.1	[e]
	IOV	+1092.2	−34.0	+620.6	−1092.2	+34.0	+620.6	[f]
	FOC	−1034.7	−14.0	+558.6	+1034.7	+14.0	+558.6	[g]
BeiDou-2	MEO	−432.1	−562.1	+1112.8	−432.1	−562.1	+1112.8	[h]
	IGSO	−402.6	−573.0	+1093.4	−402.6	−573.0	+1093.4	[i]
	GEO	−543.7	−570.4	+1093.0	−543.7	−570.4	+1093.0	[j]
QZSS	QZS-1	−1149.1	−552.9	+2685.4	+1149.1	+552.9	+2685.4	[k]
IRNSS	–	+1120.0	+436.0	−528.0	−436.0	+528.0	+1120.0	[l]

Notes:
[a] SVN 35 (ILRS, 2015d).
[b] GLONASS No. 789 and 791 (ILRS, 2015c).
[c] GLONASS-M No. 712, 713, and 716 (ILRS, 2015c).
[d] GLONASS-K1 No. 701 (ILRS, 2015e).
[e] Zandbergen and Navarro (2008).
[f] IOV-1, w.r.t. CoM of 11/2014 (ILRS, 2015b; Navarro-Reyes, 2011).
[g] FOC-1, w.r.t. CoM of 3/2015 (ILRS, 2015b; Navarro-Reyes, 2014). Values apply for FOC-1 and consider a possible CoM shift after orbit raising. Different values may apply for FOC-2 and follow-on FOC satellites.
[h] BeiDou M1, M3 (ILRS, 2015a; Yang, 2008; Zhang, 2012c).
[i] BeiDou I3, I5 (ILRS, 2015a; Zhang, 2012b).
[j] BeiDou G1 (ILRS, 2015a; Zhang, 2012a).
[k] w.r.t. CoM of 7/2012 (Nakamura and Kishimoto, 2010; Kogure, 2012).
[l] ILRS (2015f) and Ganeshan (2014).

YS-mode to properly handle the low-β regime of QZS-1 and BeiDou MEO/IGSO satellites as well as the BeiDou GEO spacecraft.

A special situation has to be faced for IRNSS, which applies a biased yaw-steering mode for better antenna coverage of the primary service area. In view of the moderate yaw, pitch, and roll biases required for this off-nadir-pointing, the standard $\mathcal{R}_{YS}$ frame is likely to also provide a reasonable approximation of the IRNSS-specific yaw-steering frame. However, only limited practical experience is available for IRNSS and further studies will, therefore, be required to justify this approximation.

4. Antenna and reflector offsets

Complementary to the discussion of satellite geometries in Section 3, the present section provides an overview of antenna phase center and LRA coordinates for the different GNSS satellites. Values are provided both in the manufacturer frame (adopted, e.g., by the ILRS and commonly used in satellite design documentation) and in the IGS-specific body frame. The different CoM offsets for modeling of GNSS and SLR observations are summarized in Tables 3 and 4, respectively.

Values given here should be considered as approximate and are mainly presented here for better understanding of the geometric characteristics. Reference values for generating and using IGS GNSS products are provided in the most recent release of the IGS ANTEX file (Schmid, 2015). This model also provides frequency-dependent phase center coordinates if available from corresponding calibration measurements. For SLR processing, reference data for all supported spacecraft are provided by the ILRS (ILRS, 2015g).

5. Summary and conclusions

The precise modeling of radiometric and laser-based distance measurements to GNSS satellites requires proper knowledge of the respective transmitter and reflector positions relative to the spacecraft CoM. Along with that comes a need for the concise definition of the spacecraft body frame and a consistent description of the satellite's orientation in space. With the growing number of Global and Regional Navigation Systems and the diversity of satellite manufacturers, widely different conventions for the designation of spacecraft axes and equipment coordinates have emerged. Within this paper, an effort has therefore been made to transparently and unambiguously document the existing coordinate system conventions for all GNSS satellites, to describe the nominal attitude control laws of these satellites, and to compile reference values of the GNSS antenna and LRA coordinates.

On top of this, an IGS-specific convention for the labeling of spacecraft axes is introduced as an alternative to the manufacturer-specific systems. To the extent possible, the application of this convention enables a uniform description of the nominal (yaw-steering) attitude across all

GNSS constellations and spacecraft brands. Limited exceptions such as the orbit-normal mode employed by individual QZSS and BeiDou satellites or the biased yaw-steering mode of IRNSS are identified and described.

The body axes conventions introduced here offer a common standard for IGS product generation and data exchange. Among others, they form the basis for the provision of multi-GNSS transmit antenna information in the IGS ANTEX model. Furthermore, they enable the widest possible harmonization and simplification of GNSS attitude models for antenna phase center and phase wind-up modeling in user software for precise point positioning.

Acknowledgments

The authors would like to thank all individuals and institutions that have provided background information and illustrations for this publication. Their help is greatly appreciated. Particular thanks go to H. Fruehauf, K. Kovac and W. Marquis for their valuable support on various blocks of GPS satellites.

References

Bar-Sever, Y.E., 1996. A new model for GPS yaw attitude. J. Geod. 70 (11), 714–723. http://dx.doi.org/10.1007/BF00867149.

Bar-Sever, Y., 1997. Information regarding Block IIR modeling. IGSMAIL-1653, IGS Central Bureau, Pasadena. Last accessed 2015/01/03. URL <http://igscb.jpl.nasa.gov/mail/igsmail/1997/msg00151.html>.

Degnan, J.J., Pavlis, E.C., 1994. Laser ranging to GPS satellites with centimeter accuracy. GPS World 5 (9), 62–70.

Dilssner, F., 2010. GPS IIF-1 satellite, antenna phase center and attitude modeling. Inside GNSS 5 (6), 59–64.

Dilssner, F., Springer, T., Gienger, G., Dow, J., 2011. The GLONASS-M satellite yaw-attitude model. Adv. Space Res. 47 (1), 160–171. http://dx.doi.org/10.1016/j.asr.2010.09.007.

Dorsey, A.J., Marquis, W.A., Fyfe, P.M., Kaplan, E.D., Wiederholt, L.F., 2006. GPS system segments. In: Kaplan, E.D., Hegarty, C.J. (Eds.), Understanding GPS – Principles and Applications, 2nd Edition. Artech House, pp. 67–112.

Dow, J.M., Neilan, R.E., Rizos, C., 2009. The International GNSS Service in a changing landscape of Global Navigation Satellite Systems. J. Geod. 83 (3–4), 191–198. http://dx.doi.org/10.1007/s00190-008-0300-3.

Ebert, K., Oesterlin, W., 2008. Dynamic yaw steering method for spacecraft; European patent specification EP 1526072B1.

Fateev, A.V., Emelyanov, D.V., Tentilov, U.A., Ovchinnikov, A.V., Lukyanenko, M.V., 2013. Algorithms of the course corner definition of the space vehicle GLONASS on the sites of the anticipatory turn on the board and in the equipment of the consumer for the calculation of the aerial phase center (in Russian). Vestnik SibGAU, Bulletin of the Siberian State University named after M.F. Reshetnev 4 (50), 198–202. URL <http://www.vestnik.sibsau.ru/images/vestnik/ves450.pdf>.

Fateev, A.V., Emelyanov, D.V., Tentilov, U.A., Ovchinnikov, A.V., 2014. Passage of special sites of the orbit by the navigating space vehicle of system GLONASS (in Russian). Vestnik SibGAU, Bulletin of the Siberian State University named after M.F. Reshetnev 4 (56), 126–131. URL <http://www.vestnik.sibsau.ru/images/vestnik/vestnik%204_56.pdf>.

Fatkulin, R., 2015. GLONASS satellite geometry and attitude models, eMail to O. Montenbruck, 2015/04/20.

Feltens, J., 1991. Nicht-gravitative Störeinflüsse bei der Modellierung von GPS-Erdumlaufbahnen (Ph.D. thesis). TH Darmstadt. Deutsche Geodät. Kommission, Bayer. Akad. Wiss., München, vol. C371.

Fisher, S.C., Ghassemi, K., 1999. GPS IIF – the next generation. Proc. IEEE 87 (1), 24–47. http://dx.doi.org/10.1109/5.736340.

Fliegel, H.F., Gallini, T.E., Swift, E.R., 1992. Global Positioning System radiation force model for geodetic applications. J. Geophys. Res. 97 (B1), 559–568. http://dx.doi.org/10.1029/91JB02564.

Fruehauf, H., 2014. The development of the GPS system 1964 to 1978. In: Stanford PNT Symposium. 28–30 Oct 2014, Stanford, CA, pp. 1–42. URL <http://scpnt.stanford.edu/pnt/PNT14/2014_Presentation_Files/4.Rev.B-GPS_System_Development-Oct_2014.pdf>.

Ganeshan, A.S., 2014. IRNSS attitude and LRA offsets; eMail to O. Montenbruck, 2014/11/07.

Ganeshan, A.S., 2015. priv. comm. to O. Montenbruck, 2015/02/09-10.

Guo, J., Zhao, Q., 2014. Analysis of precise orbit determination for Beidou satellites during yaw maneuvers. Presented at China Satellite Navigation Conference (CSNC) 2014, Wuhan, 22 May 2014.

Han, C., Yang, Y., Cai, Z., 2011. BeiDou Navigation Satellite System and its time scales. Metrologia 48 (4), S213–S218. http://dx.doi.org/10.1088/0026-1394/48/4/S13.

Hauschild, A., Steigenberger, P., Rodriguez-Solano, C., 2012. QZS-1 yaw attitude estimation based on measurements from the CONGO network. Navig. J. ION 59 (3), 237–248. http://dx.doi.org/10.1002/navi.18.

Ilcev, D.S., 2007. Cospas-Sarsat LEO and GEO: satellite distress and safety systems (SDSS). Int. J. Satell. Commun. Netw. 25 (6), 559–573. http://dx.doi.org/10.1002/sat.881.

ILRS, 2015a. COMPASS center of mass information. Last accessed 2015/04/15. URL <http://ilrs.gsfc.nasa.gov/missions/satellite_missions/current_missions/cmg1_com.html>.

ILRS, 2015b. Galileo center of mass information. Last accessed 2015/04/15. URL <http://ilrs.gsfc.nasa.gov/missions/satellite_missions/current_missions/ga05_com.html>

ILRS, 2015c. GLONASS retroreflector array position relative to CoM. Last accessed 2015/04/15. URL <http://ilrs.gsfc.nasa.gov/docs/GLONASSretroreflectorarraypositionrelativeCoM+99+102.pdf>.

ILRS, 2015d. GPS-35, -36 center of mass information. Last accessed 2015/04/15. URL <http://ilrs.gsfc.nasa.gov/missions/satellite_missions/past_missions/gp35_com.html>.

ILRS, 2015e. Information needed for GLONASS-125 CoM correction. Last accessed 2015/04/15. URL <http://ilrs.gsfc.nasa.gov/docs/glonass125_com.pdf>.

ILRS, 2015f. IRNSS-1A, -1B, -1C, -1D center of mass information. Last accessed 2015/02/20. URL <http://ilrs.gsfc.nasa.gov/missions/satellite_missions/current_missions/irna_com.html>.

ILRS, 2015g. List of supported missions. Last accessed: 2015/04/15. URL <http://ilrs.gsfc.nasa.gov/missions/satellite_missions>.

Ishijima, Y., Inaba, N., Matsumoto, A., Terada, A., Yonechi, H., Ebisutani, H.,Ukawa, S., Okamoto, T., 2009. Design and development of the first quasi-zenith satellite attitude and orbit control system. In: Proc. IEEE Aerosp. Conf. IEEE. pp. 1–8. http://dx.doi.org/10.1109/AERO.2009.4839537.

Johnson, N.L., 1994. GLONASS spacecraft. GPS World 5 (11), 51–58.

Johnston, A.G.Y., Holt, A.P., Jackson, C.D., 2008. GIOVE-A AOCS: an experience from verification to flight. In: Proc. 7th Int. ESA Conference on Guidance, Navigation & Control Systems. pp. 1–12.

Jun, X., Jingang, W., Hong, M., 2012. Analysis of Beidou navigation satellites in-orbit state. Proc. China Satellite Navigation Conference (CSNC) 2012, vol. III. Springer, pp. 111–122. http://dx.doi.org/10.1007/978-3-642-29193-7_10.

Kogure, S., 2012. QZSS antenna coordinates; eMail to O. Montenbruck, 2012/07/20.

Konrad, A., Fischer, H.-D., Müller, C., Oesterlin, W., 2007. Attitude & orbit control system for Galileo IOV. Autom. Control Aerosp. 17 (1), 25–30. http://dx.doi.org/10.3182/20070625-5-FR-2916.00006.

Kouba, J., 2009. A simplified yaw-attitude model for eclipsing GPS satellites. GPS Solut. 13 (1), 1–12. http://dx.doi.org/10.1007/s10291-008-0092-1.

Kouba, J., Héroux, P., 2001. Precise point positioning using IGS orbit and clock products. GPS Solut. 5 (2), 12–28. http://dx.doi.org/10.1007/PL00012883.

Langley, R.B., 1997. GLONASS: review and update. GPS World 8 (7), 46–51.

Mader, G.L., Czopek, F., 2001. Calibrating the L1 and L2 phase centers of a Block IIA antenna. In: Proc. ION GPS 2001. Salt Lake City, UT, pp. 1979–1984.

Marquis, W., 2014a. Block IIR s/c reference frame; eMail to O. Montenbruck, 2014/12/20.

Marquis, W., 2014b. The GPS Block IIR/IIR-M antenna panel pattern. Lockheed Martin Corp. Last accessed 2014/12/28. URL <http://www.lockheedmartin.com/us/products/gps/gps-publications.html>.

Marquis, W., Krier, C., 2000. Examination of the GPS Block IIR solar pressure model. In: Proc ION GPS 2000. ION, Salt Lake City, UT, pp. 407–415.

Marquis, W., Reigh, D., 2005. On-orbit performance of the improved GPS Block IIR antenna panel. In: Proc. ION GNSS 2005. ION, Long Beach, CA, pp. 2418–2426.

Mitrikas, V., 2005. GLONASS-M dimensions and center-of-mass correction. IGSMAIL-5104, IGS Central Bureau, Pasadena. URL <http://igscb.jpl.nasa.gov/mail/igsmail/2005/msg00027.html>.

Mitrikas, V., 2011. GLONASS-K mass, dimension and orientation. eMail to J. Ray, 2011/08/24. URL <http://acc.igs.org/glonass/GLONASS-K_mitrikas_24aug11.txt>.

Montenbruck, O., Steigenberger, P., Khachikyan, R., Weber, G., Langley, R.B., Mervart, L., Hugentobler, U., 2014. IGS-MGEX: preparing the ground for multi-constellation GNSS science. Inside GNSS 9 (1), 42–49.

Nakamura, S., Kishimoto, M., 2010. ILRS SLR mission support request form/ retroreflector information – QZS-1. 29 Jul 2010. Last accessed 2014/12/28. URL <http://ilrs.gsfc.nasa.gov/docs/ILRS_retroreflector_QZS_20100729.pdf>.

Navarro-Reyes, D., 2011. ILRS SLR mission support request form (Jun 2011) – Galileo-101 (SIC=7101) and Galileo-102 (SIC=7102). 31 Aug 2011. Last accessed 2014/12/28. URL <http://ilrs.gsfc.nasa.gov/docs/ILRS_MSR_Galileo_201106.pdf>.

Navarro-Reyes, D., 2014. Galileo FOC satellite's LRA additional information. ESA-DTEN-NG-MEM0/0017611, ESA/ESTEC, 2014/11/19. Last accessed 2015/04/15. URL <http://ilrs.gsfc.nasa.gov/docs/2014/Galileo_FOC_LRA_additional_information_signed.pdf>.

Pearlman, M.R., Degnan, J.J., Bosworth, J.M., 2002. The International Laser Ranging Service. Adv. Space Res. 30 (2), 135–143. http://dx.doi.org/10.1016/S0273-1177(02)00277-6.

Revnivykh, S., Mitrikas, V., 1998. GLONASS s/c mass and dimension. IGEXMail-0086, IGS Central Bureau, Pasadena. URL <http://igscb.jpl.nasa.gov/mail/igexmail/1998/msg00085.html>.

Rizos, C., Montenbruck, O., Weber, R., Weber, G., Neilan, R., Hugentobler, U., 2013. The IGS MGEX experiment as a milestone for a comprehensive multi-GNSS service. In: Proc. ION PNT 2013. Honolulu, HI, pp. 289–295.

Rockwell International, 1974. Proposal for space segment development of the Global Positioning System, Rockwell International, Doc. No. SD 74-SA-0014-1 1974, responding to USAF RFP F04701-74-R-0006, Apr 1974.

Rodriguez-Solano, C.J., Hugentobler, U., Steigenberger, P., 2012. Adjustable box-wing model for solar radiation pressure impacting GPS satellites. Adv. Space Res. 49 (7), 1113–1128. http://dx.doi.org/10.1016/j.asr.2012.01.016.

Rothacher, M., Schmid, R., 2010. ANTEX: the antenna exchange format, Version 1.4, 15 Sep 2010. URL <http://igs.org/pub/station/general/antex14.txt>.

Schmid, R., 2015. IGS08 ANTEX file. Last accessed: 2015/03/01. URL <http://igscb.jpl.nasa.gov/igscb/station/general/igs08.atx>.

Schmid, R., Khachikyan, R., 2012. igs08_1708.atx: Update including Block IIF-3 satellite SVN65/PRN24. IGSMAIL-6670, IGS Central Bureau, Pasadena. Last accessed 2015/02/20. URL <http://igscb.jpl.nasa.gov/pipermail/igsmail/2012/007860.html>.

Schmid, R., Rothacher, M., Thaller, D., Steigenberger, P., 2005. Absolute phase center corrections of satellite and receiver antennas. GPS Solut. 9 (4), 283–293. http://dx.doi.org/10.1007/s10291-005-0134-x.

Schmid, R., Steigenberger, P., Gendt, G., Ge, M., Rothacher, M., 2007. Generation of a consistent absolute phase center correction model for GPS receiver and satellite antennas. J. Geod. 81 (12), 781–798. http://dx.doi.org/10.1007/s00190-007-0148-y.

Steigenberger, P., Dach, R., Prange, L., Montenbruck, O., 2015. Galileo satellite antenna modeling. In: Proc. EGU General Assembly, 12–17 April 2015, EGU2015-10772.

Teunissen, P.J.G., Khodabandeh, A., 2015. Review and principles of PPP-RTK methods. J. Geod. 89 (3), 217–240. http://dx.doi.org/10.1007/s00190-014-0771-3.

Wang, W., Chen, G., Guo, S., Song, X., Zhao, Q., 2013. A study on the Beidou IGSO/MEO satellite orbit determination and prediction of the different yaw control mode. In: Sun, J., Jiao, W., Wu, H., Shi, C. (Eds.), Proc. China Satellite Navigation Conference (CSNC) 2013, vol. III. Springer, pp. 31–40. http://dx.doi.org/10.1007/978-3-642-37407-4_3.

Wübbena, G., Schmitz, M., Mader, G., Czopek, F., 2007. GPS Block II/IIA satellite antenna testing using the automated absolute field calibration with robot. In: Proc. ION GNSS 2007. Fort Worth, TX, pp. 1236–1243.

Wu, J.-T., Wu, S.C., Hajj, G., Bertiger, W.I., Lichten, S.M., 1993. Effects of antenna orientation on GPS carrier phase. Manuscr. Geod. 18 (2), 91–98.

Yang, F., 2008. COMPASS retroreflector information form. 24 Sep 2008. Last accessed 2014/12/28. URL <http://ilrs.gsfc.nasa.gov/missions/satellite_missions/current_missions/cmg1_reflector.html>.

Zandbergen, R., Navarro, D., 2008. Specification of Galileo and GIOVE space segment properties relevant for satellite laser ranging. Tech. Rep. ESA-EUING-TN/10206, iss. 3.2, 08/05/2008, ESA/ESTEC, Noordwijk.

Zentgraf, P., Fischer, H.-D., Kaffer, L., Konrad, A., Lehrl, E., Müller, C., Oesterlin, W., Wiegand, M., 2006. AOC design and test for GSTB-V2B. In: Proc. 6th ESA Guidance, Navigation and Control Systems Conf. Vol. SP 606. ESA, pp. 1–7.

Zhang, Z., 2012a. ILRS SLR mission support request form – Compass-G1. 31 Mar 2012. Last accessed 2014/12/28. URL <http://ilrs.gsfc.nasa.gov/docs/ilrsmsr_G11.pdf>.

Zhang, Z., 2012b. ILRS SLR mission support request form – Compass-I3. 31 Mar 2012. Last accessed 2014/12/28. URL <http://ilrs.gsfc.nasa.-gov/docs/ilrsmsr_I31.pdf>.

Zhang, Z., 2012c. ILRS SLR mission support request form – Compass-M3. 31 Mar 2012. Last accessed 2014/12/28. URL <http://ilrs.gsfc.nasa.gov/docs/ilrsmsr_M31.pdf>.

Zhou, S., Hu, X., Zhou, J., Chen, J., Gong, X., Tang, C., Wu, B., Liu, L., Guo, R., He, F., Li, X., Tan, H., 2013. Accuracy analyses of precise orbit determination and timing for COMPASS/Beidou-2 4GEO/5IGSO/4MEO constellation. Proc. China Satellite Navigation Conference (CSNC) 2013, vol. III. Springer, pp. 89–102. http://dx.doi.org/10.1007/978-3-642-37407-4_8.

Zumberge, J.F., 1992. JPL orbit products. in: IGSMAIL-81, IGS Central Bureau, Pasadena. Last accessed 2015/01/28. URL <http://igscb.jpl.nasa.gov/mail/igsmail/1992/msg00080.html>.